# Reconstitution of Bluetongue Virus Polymerase Activity from Isolated Domains Based on a Three-Dimensional Structural Model

Josa-marie Wehrfritz, Mark Boyce, Sahdia Mirza, Polly Roy
*Department of Infectious and Tropical Diseases, London School of Hygiene and Tropical Medicine, London WC1E 7HT, UK*

*Received 15 December 2006; revised 16 February 2007; accepted 19 February 2007*
*Published online 23 February 2007 in Wiley InterScience (www.interscience.wiley.com). DOI 10.1002/bip.20706*

**ABSTRACT:**

*Bluetongue virus (BTV) is a double-stranded RNA virus of the* Reoviridae *family. The VP1 protein of BTV is the viral RNA-dependent RNA polymerase (RdRp), which is responsible for the replication of the viral genome. Currently there is no structural information available for VP1. By manual alignment of BTV, Reovirus and other viral RdRps we have generated a model for the structure of VP1, the RdRp of BTV. The structure can be divided into three domains: an N-terminal domain, a C-terminal domain, and a central polymerase domain. Mutation of the putative catalytic site in the central polymerase domain by site-directed mutagenesis abrogated in vitro replicase activity. Each of the domains was expressed individually and subsequently partially purified to obtain direct evidence for the location of polymerase activity and the nucleoside triphosphate binding site. The nucleoside triphosphate binding site was located by showing that CTP only bound to the full-length protein or to the polymerase domain and not to either of the other two domains. None of the domains had catalytic activity when tested individually or in tandem but when all three domains were mixed together the RdRp activity was reconstituted. This is the first report of the reconstitution of a functional viral RdRp in vitro from individual domains. © 2007 Wiley Periodicals, Inc. Biopolymers 86: 83–94, 2007.*

*Keywords: RNA-dependent RNA polymerase; modeling; bluetongue virus; reconstitution; replicase*

*Correspondence to:* Polly Roy; e-mail: polly.roy@lshtm.ac.uk
Contract grant sponsor: BBSRC (UK)
This article contains supplementary material available via the Internet at http://www.interscience.wiley.com/jpages/0006-3525/suppmat



*This article was originally published online as an accepted preprint. The "Published Online" date corresponds to the preprint version. You can request a copy of the preprint by emailing the Biopolymers editorial office at biopolymers@wiley.com*

## INTRODUCTION

The RdRp is an essential protein encoded by all RNA viruses that replicate their genome via an RNA intermediate. All DNA and RNA polymerases share a similar structure, and RdRps are more similar to each other than to other polymerases. There are several crystal structures of RdRps available including those from poliovirus (PV);[1] Hepatitis C virus;[2] Rabbit Hemorrhagic Disease Virus (RHDV);[3] bacteriophage $\varphi 6$[4]; Foot and Mouth Disease Virus;[5] Bovine Viral Diarrhea Disease Virus;[6] Rhinovirus;[7] and Reovirus.[8] All adopt the typical polymerase structure of a right hand complete with fingers, palm, and thumb subdomains. Cocrystallization with nucleoside triphosphates (NTPs) or with oligonucleotides of these enzymes has mapped substrate binding sites, while the binding of divalent cations, $Mg^{2+}$ or $Mn^{2+}$, has been mapped to the catalytic sites.[3,5,6,8] The active site is at the heart of the molecule, in the centre of the palm domain, and an additional domain, N-terminal to the fingers that anchors the tips of the fingers to the thumb is present in RdRps.[3,6,8] Beyond several conserved motifs there is little primary sequence conservation among the RdRps of the RNA viruses in general, or among those of the double-stranded (ds) RNA viruses. The catalytic site is normally characterized by a GDD motif, also known as motif

C.[9–12] In addition to the GDD motif, several other less obvious sequence motifs (A, B, and D–F) have been identified from diverse virus families on the basis of primary and secondary structure analysis.[9–12]

Bluetongue virus (BTV) has a 10-segment double-stranded RNA (dsRNA) genome and has been well characterized at a molecular and structural level.[13–15] It is a member of the Orbivirus genus in the family *Reoviridae*. VP1 is the largest BTV protein at 150 kDa, and is encoded by BTV RNA segment 1. BTV VP1 has been shown to be a processive viral RdRp, synthesizing dsRNA from a single stranded (ss) RNA template in the absence of other viral proteins,[16,17] but there is currently no X-ray crystal structure data available for it. The RdRps of bacteriophage $\varphi$6 (P2) and Reovirus ($\lambda$3), for which detailed structural data are available, are potentially the most similar to VP1 as both viruses have segmented double stranded (ds) RNA genomes. The P2 protein of $\varphi$6 is small at 664 amino acids in comparison with the 1302 amino acids of VP1. P2 acts both as a replicase and a transcriptase and is able to use both ssRNA and dsRNA as templates.[4,18,19] In contrast, there is currently no experimental evidence that VP1 is able to transcribe RNA from a double-stranded template in the absence of other viral proteins. It may be that the transcriptase activity of VP1 is dependent on the presence of another BTV protein, VP6, which is a helicase protein and has the ability to unwind the dsRNA prior to transcription.[20] Reovirus $\lambda$3, which has a total of 1267 amino acids, is a similar size to BTV VP1. $\lambda$3 has a centrally placed polymerase domain (PD) and large N-terminal domain (NTD) and C-terminal domain (CTD) which form a cage around the PD holding it rigid and preventing movement during the catalytic cycle.[8] The NTD covers one side of the active site, and anchors the fingertips to the thumb. It occupies a similar position to the NTDs found in other RdRps but is considerably larger. A cap recognition site has been located on the NTD of $\lambda$3 which anchors the 5′ end of the dsRNA template during RNA replication.[8] The CTD of $\lambda$3 forms a bracelet structure with two tightly sealed circles. The opening in the centre of the bracelet forms the exit route for the nascent double stranded RNA.[8]

BTV VP1 has two GDD motifs at positions 287–289, and 763–765. Only the latter GDD motif is surrounded by the other sequence motifs (A, B, and D–F) characteristic of polymerase proteins,[10,11] which suggests that VP1 may have a single, central PD, similar to reovirus $\lambda$3.

## RESULTS

### BTV VP1 has a Central PD

As protein modeling is dependent on a strong alignment to the sequence of a known structure, polymerase modeling is hampered by low sequence homology. Initially the BTV-10 VP1 sequence was submitted to the web-based server SAM T-02 in blocks of 500 amino acid residues. Submission of the central 500 amino acid residues of VP1 produced alignments with the RdRps of two positive sense ssRNA viruses, RHDV and PV. Subsequently PSIPRED[21] was used to predict the secondary structure of VP1, and then this prediction was compared to the secondary structure assignments obtained from the X-ray crystal structures of the RHDV and PV RdRps. Further alignment of motifs A-F and secondary structure was performed manually. The final polymerase sequence alignments (Figures 1A and 1B) were submitted together to the program MODELLER,[23] to generate a spatially restrained three-dimensional model of the PD of VP1 (Figure 2A). The model has a typical polymerase structure and has the canonical structure of a right hand with "fingers" (blue), "palm" (red), and "thumb" (green). The "fingers" subdomain has three $\alpha$ helices ($\alpha$-a,d,e; supplementary information) and four $\beta$ strands ($\beta$-1,2,4,5 supplementary information). Generally most RdRps have eight $\alpha$ helices and five or more $\beta$ strands, one of which is contributed by the NTD.[1,3,5–7] The modeled PD of VP1 might therefore be missing some alpha helical structure. Also, there is a region between the NTD model and the PD model (residues 374–580), which currently remains unmodeled as sequence homology in this region is too low for reliable alignment with known protein structures. Although it is possible that VP1 may have an area of unique structure adjacent to the "fingers" subdomain, it would be surprising if it was not possible to model the complete "fingers" subdomain as this structure is well conserved between polymerases. Another possibility is that the unmodeled region belongs to the NTD.

The "palm" subdomain predicted for VP1 is composed of a four-stranded antiparallel $\beta$ sheet flanked by three $\alpha$ helices (Figure 2A, also see supplementary information). This is an arrangement universally found in polymerases. The architecture of the "palm" region is the most highly conserved structure of all known polymerases and many of its features are shared across all families of RNA and DNA polymerases.[12] It contains some of the conserved sequence motifs common to all RdRps and which are involved in nucleotide binding, phosphoryl transfer, structural integrity of the "palm" subdomain, and priming nucleotide binding.[5] Figure 2C (i) depicts a portion of the modeled PD of VP1 showing the region containing conserved sequence motifs A–D, all of which show strong structural similarity to the solved structures of other RdRps (Figure 2C, ii, iii, iv). The sequence motifs make up the highly conserved structure of the "palm" subdomain. The aspartate residues in motif C which are predicted to be responsible for divalent cation coordination are at positions

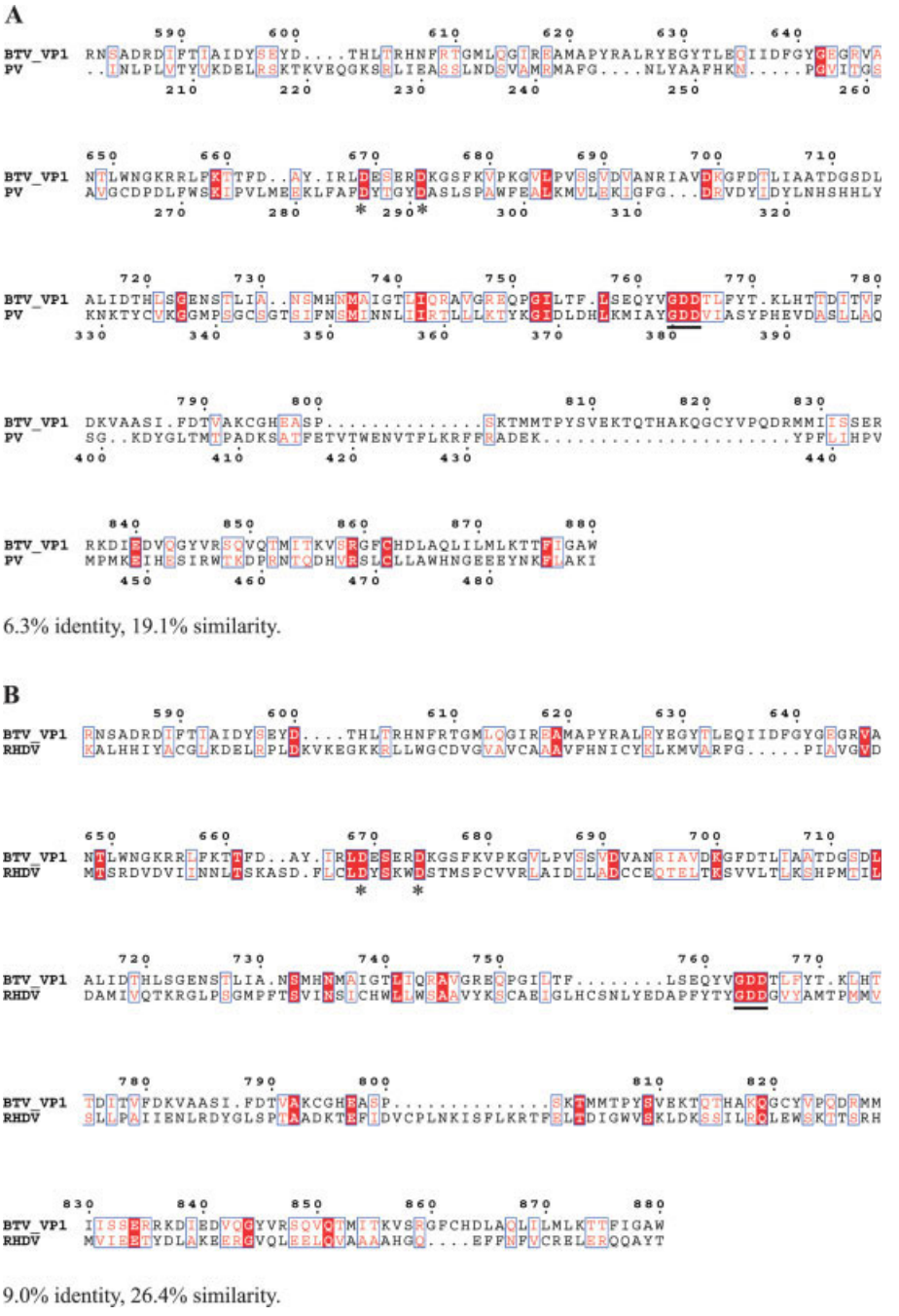


**FIGURE 1** Alignments used to generate the polymerase domain model of BTV VP1. The alignment of BTV VP1 polymerase domain with poliovirus RdRp (A) or with RHDV RdRp (B). Pairwise alignments derived from the original alignment of all three sequences are shown for clarity. Identical residues are on a red background, and similar residues are in red font. Similarity was defined using ESPript 2.2,[22] with a similarity score of 0.8 and using physicochemical properties of side chains as the criteria for similarity. Motif A is indicated with asterisks. Motif C is underlined.

764 and 765 (Figure 2B). Two additional aspartate residues believed to be involved in either metal ion coordination or the binding of NTPs are positioned in Motif A at residues 669 and 674 in the model[7] (Figure 1).

The "thumb" subdomain of modeled VP1 has three α-helices linked by loops. The "thumb" subdomain of RdRps generally have four or more α-helices that are preceded by a short $\beta$ strand that is located between the "palm" and the "thumb"

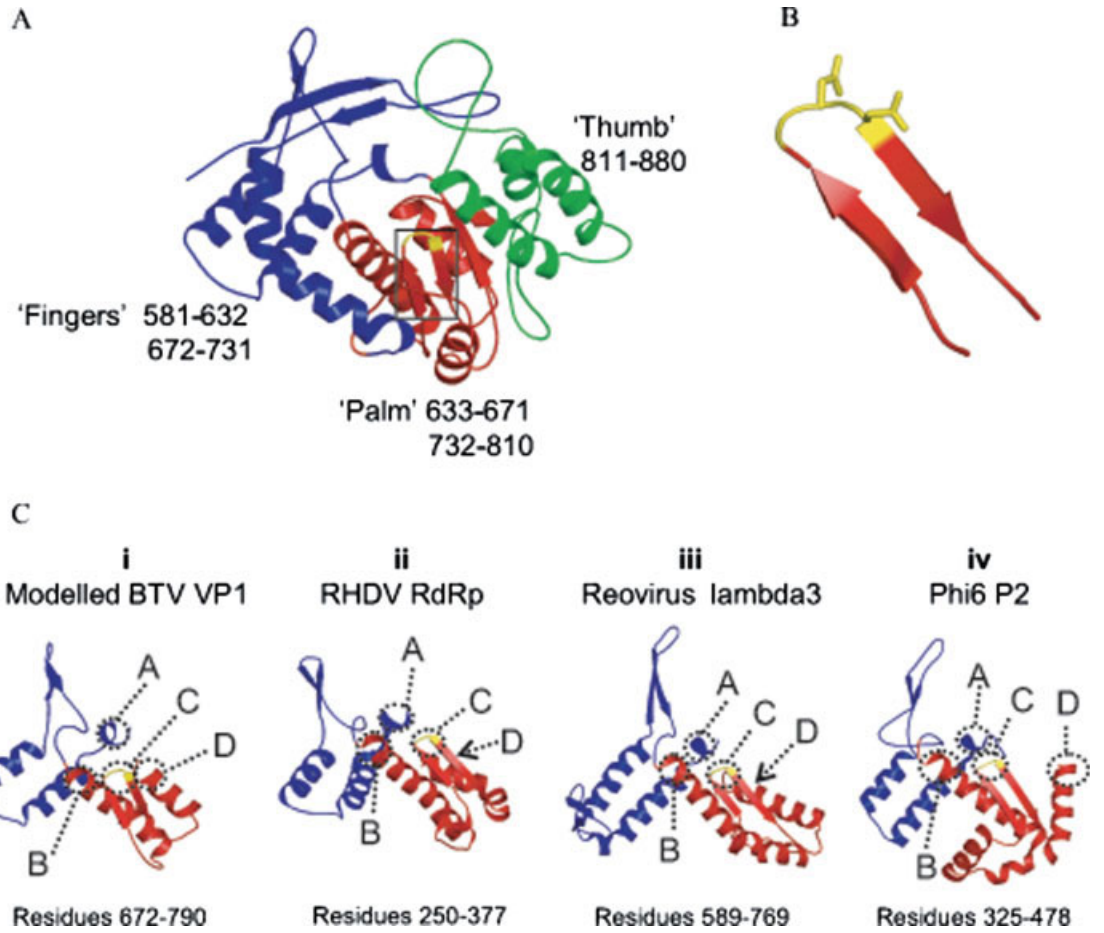


**FIGURE 2** Model of the polymerase domain of VP1 and comparison of the modeled structure at the conserved motifs A–D with the solved structures of other polymerases. (A) The polymerase domain model is based on the complete X-ray crystal structures of the RdRps of two ssRNA viruses, poliovirus and RHDV. The "fingers" subdomain is in blue, the "palm" subdomain is in red and the "thumb" subdomain is green. Motif C in the "palm" subdomain is in yellow. (B) Expansion of the boxed region in panel A, showing the motif C (GDD motif) in yellow at residues 763–765. Amino acid side chains are depicted for motif C only. (C) A comparison of the model of BTV VP1 proximal to motifs A–D with the corresponding regions of the solved structures of RdRps. The regions of structure that correspond to the sequence motifs A–D are circled. Motif C is colored yellow. (i) modeled BTV VP1; (ii) RHDV RdRp; (iii) Reovirus $\lambda 3$, and (iv) $\varphi 6$ P2.

subdomains.[3,8] In VP1 there is a gap in the PD alignment, implying that this $\beta$-strand is missing. The "thumb" of $\lambda 3$ polymerase only has three helices and it is possible that VP1 resembles $\lambda 3$ in the region of the "thumb" subdomain.

## VP1 has Amino-Terminal and Carboxy-Terminal Domains Similar to Reovirus λ3

Reovirus $\lambda 3$ is the only RdRp from the same virus family as BTV for which the structure has been solved, and was used to model the amino-terminal and carboxy-terminal regions of BTV VP1.[8] Multiple Orthoreovirus and Orbivirus sequences were submitted to ClustalW to produce an alignment. Secondary structure predictions were used to make manual adjustments to the ClustalW sequence alignments. The model of the NTD is a crescent shaped alpha beta protein (Figure 3), which is predicted to fit over the PD model and thus anchor the fingertips to the thumb. A comparison of the NTD model with the region of reovirus $\lambda 3$ used to derive it gives a root mean square deviation (RMSD) value of 0.9 Å, demonstrating a high degree of structural similarity. At the level of primary sequence 9.1% of residues were identical to reovirus $\lambda 3$ while 19.4% residues were similar (Figure 4A). However, unlike the $\lambda 3$, no obvious cap recognition residues in VP1 were detected from the alignment used.

As mentioned previously, there is a region that it was not possible to model. This unmodeled region may indicate a

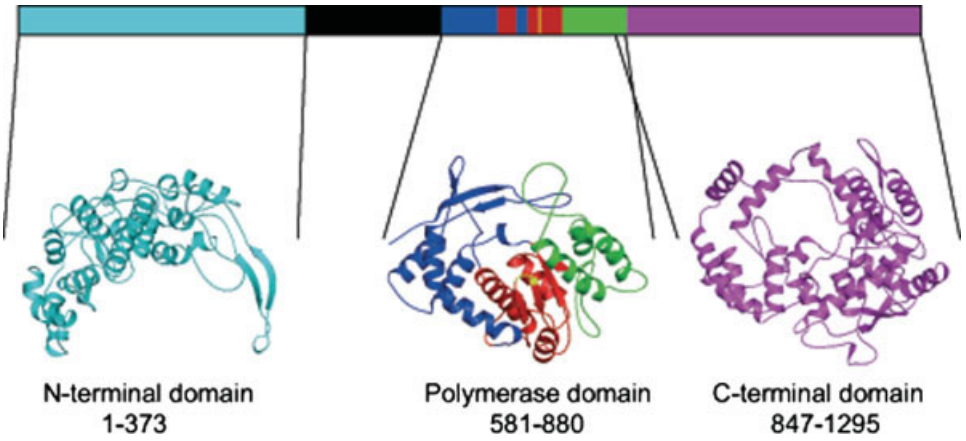


**FIGURE 3** Modeled and cloned regions of BTV VP1. (A) The NTD modeled from amino acid residues 1–373 is shown in cyan. The PD model covers amino acid residues 581–880. The "fingers" subdomain is blue, the "palm" subdomain is red, and the "thumb" subdomain is green. The CTD modeled from amino acid residues 847–1295 is in magenta. The CTD model overlaps with the "thumb" subdomain of the PD model.

binding site for VP4, the BTV capping enzyme, alternatively it may be a site at which VP1 interacts with VP6, a protein which is absent in reovirus. Another possibility is that it is the point at which VP1 and VP3 interact, anchoring VP1 to the interior of the BTV subcore.

The modeled CTD of VP1 has a bracelet structure like that of λ3 (Figure 3). In λ3 this bracelet structure forms a pore through which the newly formed genomic dsRNA exits the polymerase. The model of the CTD has a RMSD value of 0.72 Å when compared with the corresponding region of reovirus λ3, demonstrating a high degree of structural similarity. At the level of primary sequence 23.1% similar residues and 11.3% identical residues were shared by the two proteins (Figure 4B). The VP1 polymerase CTD has 20 α helices and 6 β strands as does the C-terminal region of λ3. From our alignment and modeling data we believe that BTV VP1 and λ3 have very close structural similarity in this region of the molecule and that the CTD of BTV VP1 forms an exit pore for the nascent dsRNA. The model of the VP1 CTD overlaps with part of the "thumb" subdomain of the VP1 PD such that the last two α-helices of the "thumb" subdomain are the first two α helices in the model of the CTD (Figure 3). Following these α helices there is an anti-parallel β sheet composed of two β strands followed by a short α helix which raises the possibility that the "thumb" subdomain modeled for VP1 actually has a total of four α-helices like many other polymerases.

The initial search of the SAM T-02 server database, using the central portion of BTV VP1, did not identify the equivalent regions of reovirus λ3 or bacteriophage φ6 P2, the structures of which are known.[4,8] Subsequently, a search of the FUGUE server database[24] with the full-length VP1 recovered an alignment spanning the entire length of the VP1 protein with the sequence of reovirus λ3, suggesting that the PD of VP1 could also be modeled on λ3. The parts of VP1 that could be modeled from this alignment were examined and the NTD and CTD domains were found to be similar to the models already obtained. The alignment suggested that the PD domain could also be modeled by aligning the sequence of VP1 with λ3. The modeled regions that were obtainable from this alignment showed a polymerase-type structure similar to the model already obtained and similar to the PD of λ3 (data not shown). A comparison of the RMSD value between the complete PD model derived from PV and RHDV and the PD of reovirus λ3 gave a value of 2.0 Å deviation. A structural alignment of the modeled PD and the solved PD of λ3 was carried out using the program SHP[25] and the sequence alignment of structurally equivalent residues is shown in Figure 5.

## Mutation of the GDD Motif at Amino Acids 763–5 Abrogates the Replicase Activity of BTV VP1

The signature motif of the catalytic site of polymerases is normally characterized by a GDD motif which is commonly located within the centre of the palm domain. The putative PD of VP1 comprises the residues 581–880 and a GDD motif (aa763–765) is located in this domain. To obtain biological evidence that this motif is functional we have generated two recombinant baculoviruses, one expressing amino-terminal 6His-tagged mutant VP1 $DD_{764–765}AA$ and the other equivalent 6His-tagged wild-type VP1. Both tagged proteins were then purified and analyzed by SDS-PAGE (Figure 6A). Both wild-type VP1 (Figure 6A, lane 4) and VP1 $DD_{764–765}AA$ (Figure 6A, lane 2) were purified to near-homogeneity. To assess the effect of altering the GDD motif to GAA on dsRNA

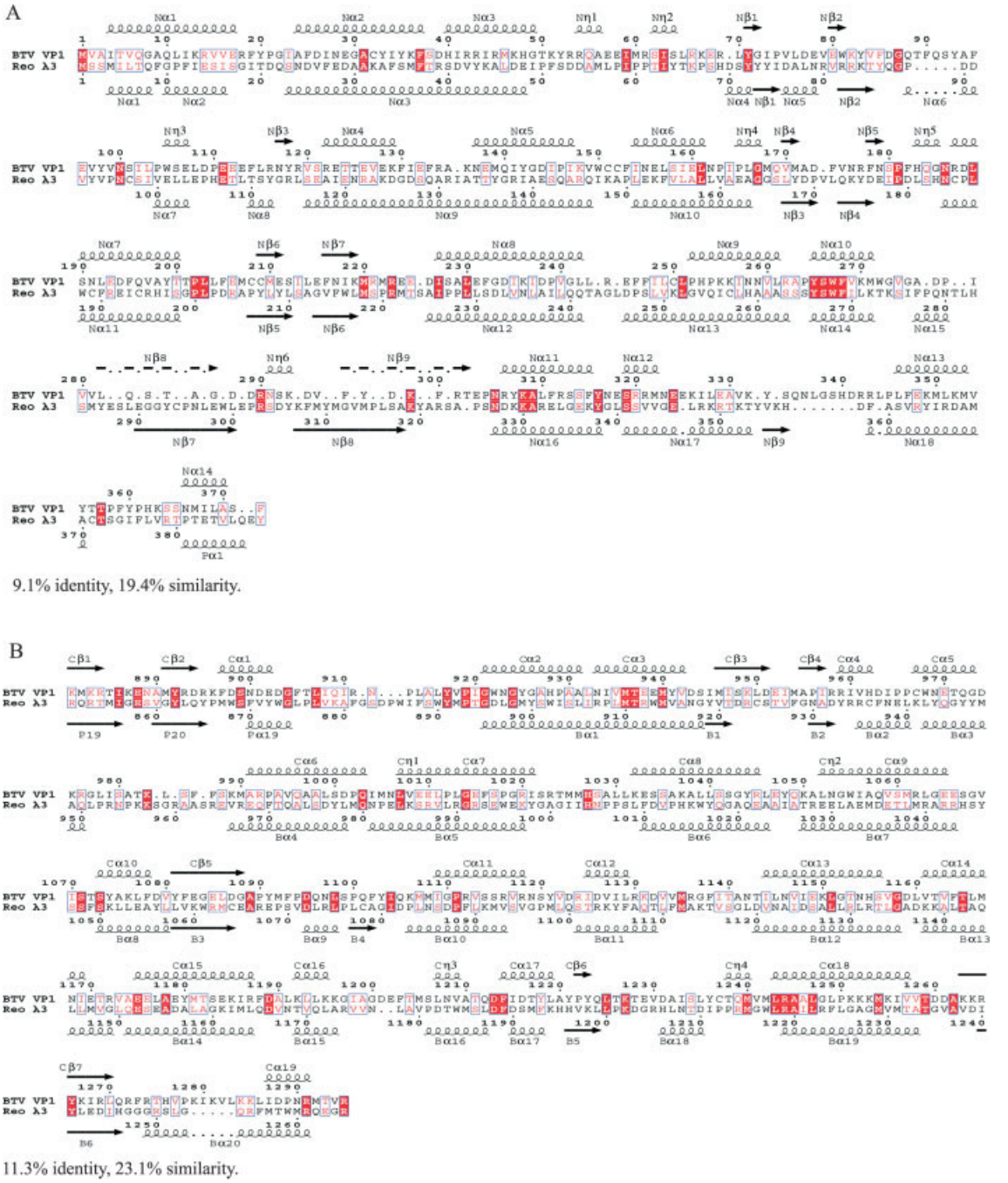


**FIGURE 4** Alignment of structurally equivalent residues between the NTD and CTD models and the corresponding regions of λ3. (A) Alignment of the NTD model of BTV VP1 with the structural template (reovirus λ3). (B) Alignment of the CTD model of BTV VP1 with the structural template. Similar and identical residues are shaded as described for Figure 1.

synthesis, wild-type VP1 and mutant VP1 $DD_{764–765}AA$ were assayed for synthesis of dsRNA using a ssRNA template in an in vitro replicase assay system published previously.[17] Products of the replicase assay were analyzed on a 9% polyacrylamide gel (Figure 6B). Wild-type VP1 synthesized segment 10 dsRNA from a segment 10 ssRNA transcript template (Figure 6B, lane 3), demonstrating the processive replicase activity of VP1. However, the mutant VP1 ($DD_{764–765}AA$) did not synthesize any detectible dsRNA (Figure 6B, lane 2), even after a 10-fold longer exposure (data not shown). The

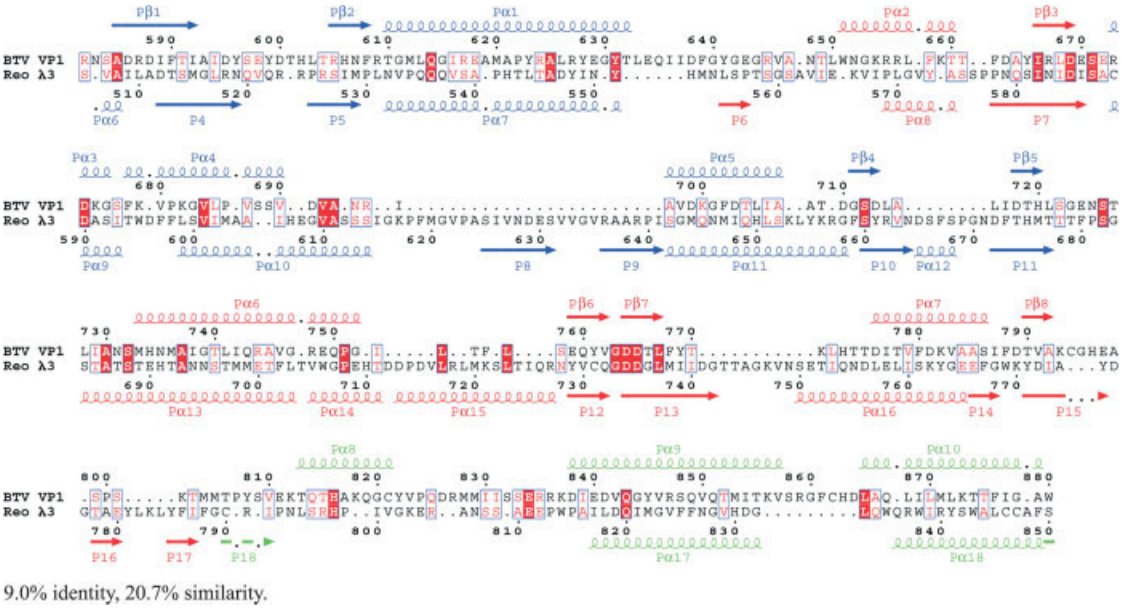


**FIGURE 5** Alignment of structurally equivalent residues of the polymerase domains of BTV VP1 and reovirus λ3. Similar and identical residues are shaded as described for Figure 1. Secondary structure elements are colored as for Figure 2.

mutation of the conserved GDD motif in the putative PD of VP1 abrogated the replicase activity of VP1, demonstrating the necessity of aspartate residues 764–765 for the processive replicase activity. This is consistent with the modeling of residues 581–880 of VP1 as the PD, and specifically the identification of residues 763–765 as motif C.

## The Domains of BTV VP1 can be Individually Expressed in Soluble Form in *E. coli*

The modeling data indicated that BTV VP1 could be divided into three domains: an N-terminal domain; a polymerase domain; and a C-terminal domain (Figure 3). We wanted to determine if these domains are biologically functional domains. To this end based on the model, three constructs were designed to express each domain separately in *E. coli*. The expression of each domain was then analyzed by SDS-PAGE followed by Coomassie staining which showed bands of the predicted size (Figure 7A). The identity of the expressed VP1 domains was confirmed by Western blotting (Figure 7A).

Each domain was more soluble when expressed at 30°C than at 37°C (data not shown) and thus 30°C was routinely used for expression. Fractionation of the cells expressing the

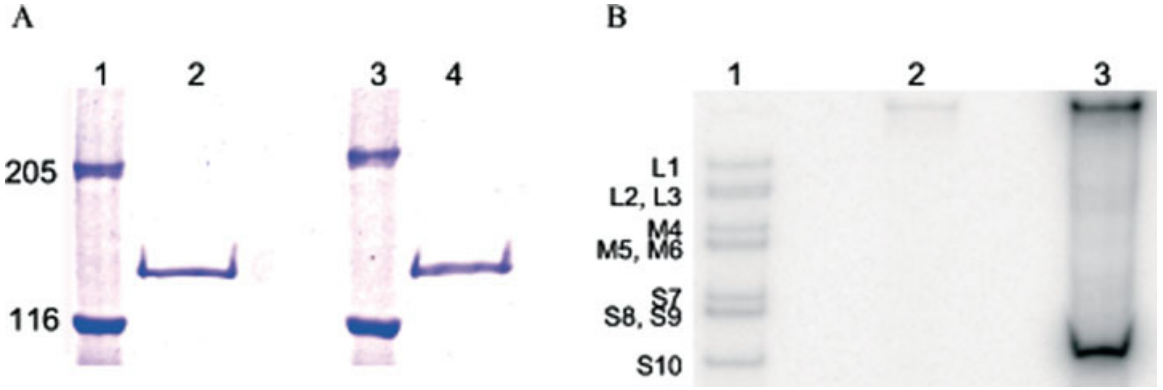


**FIGURE 6** Purification of wild-type and mutant VP1 protein and replicase activity. (A) SDS-PAGE of purified wild-type His-VP1 and His-VP1 $DD_{764–765}AA$ mutant. Lanes 1 and 3, protein size markers (kDa); lane 2, VP1 mutant; lane 4, wild-type VP1. (B) Replicase assay of wild-type and mutant $DD_{764–765}AA$ VP1 proteins. Lane 1 $^{32}P$-labeled BTV-10 genomic dsRNA; lane 2, replicase assay products using His-VP1 $DD_{764–765}AA$; lane 3, replicase assay products using wild-type His-VP1.

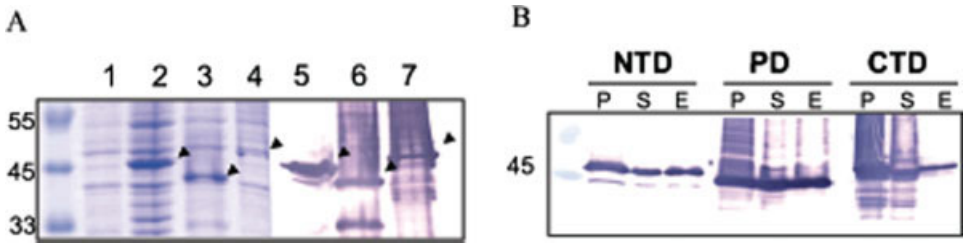


**FIGURE 7** Expression and purification of VP1 fragments. (A) VP1 fragments were expressed in *E.coli* strain HMS174 (DE3) and the total cell extracts were electrophoresed on a 12% SDS-polyacrylamide gel followed by staining with Coomassie blue. Lane 1, empty vector control; lane 2, NTD; lane 3, PD; lane 4, CTD. Lanes 5–7 are the Western blot of the equivalent gel developed using a commercial anti-polyhistidine antibody; lane 5, NTD; lane 6, PD; lane 7, CTD. Arrowheads indicate positions of VP1 fragments. (B) Western blot of purified VP1 fragments electrophoresed on a 12% SDS-polyacrylamide gel. *E.coli.* cells were lysed by sonication and the VP1 fragments subsequently partially purified by a standard cobalt affinity chromatography as described in the text. The lane marked "P" is the pellet from the lysed cells; S is the soluble lysate; and the lane marked "E" is the material eluted from the cobalt beads. Position of size markers in kDa indicated on the left side.

domains, when analyzed, showed that the majority of each synthesized protein was in the pellet fraction (Figure 7B, lanes marked "P"); however, there was also some protein present in the soluble fraction (Figure 7B, lanes marked "S") that could be purified on cobalt resin (Figure 7B, lanes marked "E") although both the final yield and purity of the recovered protein were not very high.

## The PD of BTV VP1 Binds NTP

Since NTP binding is an essential property of any RdRp, we determined which of the VP1 domains bound NTPs, using full-length VP1 as a positive control. NTP binding was tested by incubating each VP1 domain with oxidized [$\alpha$-$^{32}$P] CTP, as described in the Materials and Methods. To determine whether VP1 and the VP1 domains had covalently coupled CTP, the reaction products were analyzed by gel electrophoresis and visualized by autoradiography. A strong 150-kDa radioactive band was detected when full-length VP1 was used in the reaction (Figure 8, lane 1). There were also additional smaller but weaker radioactive bands present which were probably due to nonspecific binding of CTP. Of the three VP1 domains only the 45-kDa PD fragment of VP1 was bound to the radiolabeled CTP (Figure 8, lane 4). The other two VP1 fragments did not produce any radiolabeled band at the correct positions in the gel indicating that these two VP1 fragments did not have NTP binding sites. In contrast, the PD fragment bound CTP very strongly and had a higher signal than that of the full-length VP1 when an equivalent amount of protein was used in each reaction.

This result provides further evidence that GDD $_{763–765}$ in the PD is the catalytic site and not GDD$_{287–289}$ in the amino-terminal domain. It also indicates that a substantial amount of the soluble PD protein expressed in *E.coli* is correctly folded.

## The Individually Expressed Domains of BTV VP1 Reconstitute to Form an Active Polymerase

We have previously shown that full-length VP1 is able to synthesize dsRNA from a ssRNA template in vitro.[17] To determine whether the PD was sufficient for the synthesis of dsRNA it was tested in the same replicase assay, using BTV segment 10 ssRNA as a template. When the PD alone was tested no discrete product band was generated (Figure 9, lane 5). Replicase activity was also not recovered when the PD was mixed with either the NTD or the CTD (Figure 9, lanes 8–9).

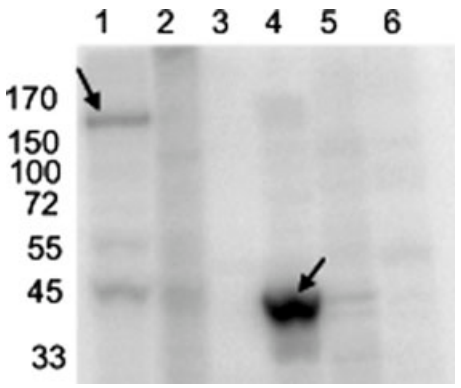


**FIGURE 8** NTP labeling of VP1 fragments. Fragments were incubated with [$\alpha$-$^{32}$P] CTP and bound nucleotides were covalently coupled before the fragments were electrophoresed on a 12% SDS-polyacrylamide gel. Lane 1, full-length VP1, purified from insect *Sf*9 cells; lane 2, *Sf* 9 cell extract; lane 3, NTD; lane 4, PD; lane 5, CTD; lane 6, bacterial cell extract. Arrows indicate the major $^{32}$P-CTP labeled bands. Position of size markers in kDa indicated on the left side.

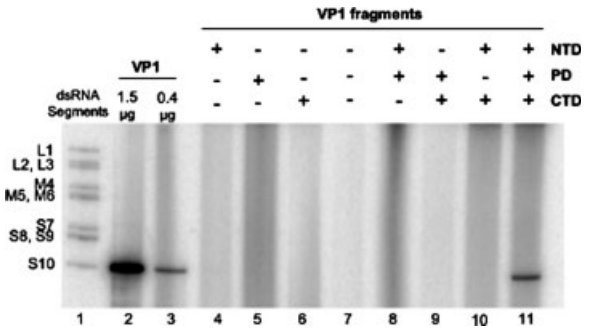


**FIGURE 9** Replicase activity of VP1 fragments. Each of the fragments was tested for replicase activity as described in the text. $^{32}$P-labeled BTV-10 genomic dsRNA markers (lane1). Positive controls for the replicase assay were purified VP1 (lane 2) or partially purified VP1 (lane 3) which was at a similar concentration and purity to the fragments. The inclusion or omission of each of the VP1 domains is indicated by a "+" or "−", respectively. One microgram of protein was used when assaying VP1 fragments individually (lanes 4–6), and 500 ng of each purified VP1 fragment was used when assaying mixtures of two or three domains (lanes 8–11). Lane 7 is an empty vector control and contains the contaminating *E.coli* proteins that were bound to and subsequently eluted from the cobalt resin during purification.

All possible permutations of the three VP1 domains were tested individually and together for replicase activity, and only when all three domains were mixed was dsRNA synthesized from the ssRNA template (Figure 9, lane 11). This indicates not only that each domain was correctly folded, but also that all three domains are required for processive RdRp activity.

An extended PD fragment (PD+) which overlapped with part of the C-terminal fragment was also constructed and tested in isolation for replicase activity (data not shown). Like the original PD fragment it also did not show any replicase activity. This fragment was not tested in the reconstitution experiment because it overlapped with part of the CTD and it was expected that this overlap would interfere with the reconstitution of the enzyme.

## DISCUSSION

Protein modeling has become a useful tool in understanding protein structure and function. However, it must be remembered that a protein model is merely theoretical unless it can be confirmed by experimental evidence. The combined approach of modeling supported by experimental results can be powerfully used to further our understanding of a protein molecule.

Database searches found that the central region of the BTV polymerase protein VP1 sequence has similarity with two other RdRps (from ssRNA viruses) and that the N-terminal and C-terminal regions of BTV VP1 have similarity with the RdRp of reovirus, a dsRNA virus of the same virus family. The polymerase protein of BTV was modeled and this model was used to identify three domains, one of which is the putative PD and which is located in the middle of the VP1 sequence. The experimental data obtained from a mutant VP1 protein, in which the aspartate residues of the catalytic site were mutated to alanine residues, confirmed that this domain is indeed the active domain of the protein and possesses the GDD catalytic site. This is consistent with the model of this domain which predicts folding into a typical "right hand" polymerase structure.

The reconstitution of polymerase activity from mixing the purified, soluble, domains predicted from the model supports the hypothesis that it is a good indication of the folding of the protein. Although in this report the mechanism of reconstitution of the domains has not been fully elucidated, it is logical to speculate that specific surface contacts form between the domains irrespective of whether the polypeptide backbone is continuous. $\lambda 3$ of reovirus has a $\beta$ strand that belongs to the NTD but which contacts all three domains, wrapping around the entire protein as it does so. This structure has been modeled into the NTD of VP1 but it is not entirely clear whether it is actually present as it seems unlikely that this strand would be able to reconstitute in vitro, wrapping itself around all three domains. The N-terminal His-tags were not cleaved from the VP1 fragments prior to reconstitution in the activity assay. Although the lack of interference of these tags is surprising, it indicates that the N-termini of the three fragments cannot be intimately involved in either the reconstitution or replicase activities.

SARS-Coronavirus polymerase cleaves naturally into segments when expressed in *E. coli.* It has a C-terminal PD which is able to remain bound to the N-terminal region of the protein after proteolysis, and during further purification.[26] Like BTV VP1, the polymerase region is unable to catalyze RNA polymerization alone and an NTD is also required for catalytic activity. Full-length VP1 has been expressed and purified from insect cells and well characterized.[17] Unlike the SARS protein there is no clear natural breakdown of purified full-length VP1 into fragments, which suggests that the links between the domains are either not surface exposed or do not contain cleavage sites.

Influenza RNA polymerase is composed of three subunits, PB1, PB2, and PA, all of which are necessary for a functional enzyme.[27,28] The subunits can be individually expressed in baculovirus and reconstituted into a functional polymerase enzyme by mixing them in a urea solution and then dialyzing them against a reconstitution buffer.[27] Protein–protein interactions between the individual polymerase subunits have been identified, suggesting that PB1 is the core of the polymerase complex. The N-terminal region of PB1 interacts with the C-terminal region of PA, while the C-terminal

region of PB1 interacts with the N-terminal of PB2 subunit. No direct protein–protein interactions have been demonstrated between PB2 and PA. In a separate study, PA-PB1 heterodimers were expressed separately from PB2 monomers and reconstitution of the functional enzyme was performed by solid phase assembly or by simply mixing the heterodimer with the monomer in solution.[28]

As far as we are aware our reconstitution of VP1 from three protein fragments, or domains, is unprecedented and we are not aware of any other RNA polymerase for which this has been demonstrated (although a similar study has been carried out on phospholipase C-$\beta_2$[29]). Our continuing studies are currently concerned with proving the role of direct protein–protein interaction in the reconstitution mechanism but at the time of writing we are unable to rule out the involvement of the single stranded RNA template in bringing the three fragments together to act sequentially or in concert.

BTV VP1 is the largest of the *Reoviridae* RdRps, with 1302 amino acid residues,[30] whereas the Reovirus RdRp has 1267[8] and the Rotavirus RdRp has 1088.[31] VP1 clearly has some structure that is not present in either of these other two family members which may explain why there is a section of VP1 that we have not been able to model. Despite the evidence that the entire structure is involved in RNA replication and transcription it is still not entirely clear why such a large structure is necessary. The P2 protein of bacteriophage $\varphi$6 efficiently replicates and transcribes viral RNA and is able to unwind dsRNA yet it is a fraction of the size of any of the *Reoviridae* RdRps at 664 amino acids. It is interesting that unlike the bacteriophage, members of the family *Reoviridae* found it necessary to evolve such bulky enzymes.

Although we have shown the involvement of the PD domain in the polymerase activity of VP1 protein, it is not yet clear what the functions of the VP1 NTD and CTD are. If the analogy with $\lambda$3 is correct, these domains form part of the functional protein, contributing to template recognition and exit of the nascent RNA strands. These domains are also likely to form attachment points for the structural protein VP3 and the capping enzyme VP4 both of which are closely associated with VP1 in the virus particle.[32] The interaction of the VP1 domains with other BTV proteins will be the subject of our future studies in addition to better understanding of the role of the NTD and CTD of VP1 in virus replication.

## MATERIALS AND METHODS

### Virus

All of the experimental and theoretical work described in this manuscript was carried out using BTV serotype 10 (BTV-10).

### Modeling

The SAM T-02 server (http://www.cse.ucsc.edu/research/compbio/) was used to search for possible structural alignments. ClustalW (www.ebi.ac.uk/clustalw/)[33] multiple sequence alignment of Orbivirus RdRp sequences (BTV serotypes 2, 8, 10,11, and 17; Chuzan virus; Saint Croix river Virus; African horse sickness virus) with Reovirus RdRp sequence was also used to help create a suitable alignment. Secondary structure prediction was performed using PSIPRED (bioinf.cs.ucl.ac.uk/psipred/).[21] Final adjustment to the alignment was done manually prior to submitting the alignment to MODELLER (salilab.org/modeller/).[23] Graphics were produced using PyMOL$^{TM}$ (DeLano Scientific LLC). Structures were aligned using SHP[25] and this data was used to draw the sequence alignment with ESPript.[22] The secondary structural elements for VP1 were defined by DSSP,[34] and those for $\lambda$3 were taken from Tao et al.[8]

### Mutagenesis of the GDD Motif of VP1

To determine whether the GDD motif at amino acid residues 763–765 is required for polymerase activity the aspartate residues were mutated to alanine residues so that Mg2+ ion coordination would no longer be possible. The GDD sequence at amino acid residues 763–765 was altered to GAA by the method of Weiner et al.[35] using a subcloned 2.8 kb *Bgl*II fragment of VP1. The following 5′ phosphorylated oligonucleotide primers were used: 5′CGGACCAATACGTGGGGGCCGCTACACTGTTTTACACAAAACTAC3′ and 5′ GTAGTTTTGTGTAAAACAGTGTAGCGGCCCCCA CGTATTGTTCCG3′. Clones were screened for the presence of the introduced mutation by sequencing, and the absence of incidental mutations was confirmed by the complete sequencing of the 2.8-kb *Bgl*II VP1fragment. The wild-type 2.8-kb *Bgl*II VP1fragment in the full-length VP1 clone pDT10.1 was replaced with the equivalent *Bgl*II fragment containing the $DD_{764–765}$AA mutation, to produce the $DD_{764–765}$AA mutant clone pDT10.1GAA. The baculovirus transfer vector pAcYM1[36] was modified by insertion at the *Bam*HI site of a dsDNA oligonucleotide encoding an amino-terminal 6His tag generating pAcYM16His. Wild-type VP1 from pDT10.1 and $DD_{764–765}$AA mutant VP1 from pDT10.1GAA, were subcloned into pAcYM16His to generate p6HisVP1 and p6HisVP1GAA.

### Generation of Recombinant Baculoviruses Containing Wild-Type VP1 or VP1 DD764–765AA

Recombinant baculoviruses were generated from p6HisVP1 and p6HisVP1GAA using linearized bacmid BAC10:KO1629 (the kind gift of Dr Ian Jones, Reading University).[37] Briefly, insect *Sf*21 cells were cotransfected with *Bsu*36I-linearized BAC10:KO1629 and either p6HisVP1 or p6HisVP1GAA. Recombinant baculoviruses were plaque purified and screened for VP1 expression by nickel affinity chromatography using HIS-Select TM Nickel Affinity Gel (Sigma).

### Purification of Wild-Type VP1 or VP1 DD764–765AA

*Sf*9 cells were infected with recombinant baculoviruses containing VP1 or VP1DD764–765AA at an MO1 of 1 for 72 h. Infected cell pellets were resuspended in 50 m*M* NaH2PO4 pH 8.0, 100 m*M* NaCl, 10% glycerol. The cells were lysed by adding NP-40 to a final concentration of 0.5% (v/v) and the expressed protein was purified from the cell lysates by standard nickel affinity chromatography as

described previously.[17] Eluates containing VP1 proteins were made to a final concentration of 1 m*M* DTT and stored at 4°C.

## Construction of Plasmids Containing the VP1 Domains

To test whether the PD could function normally without the NTD and CTDs, fragments containing the 5′, middle, and 3′ sections of the BTV-10 L1 gene were amplified by PCR from a cDNA clone using primer pairs, 5′ATCGGGATCCAGTCGCAATCACCGTGCAAGGT3′ and 5′ATCGGGATCCTTAGCAATCAGCTGCGTCCATC3′ (NTD); 5′ATCGGGATCCATTCCGTAACTCTGCCGATCGC3′ and 5′ATCGGGATCCTTACTTTCTGTCGCGATACATCGC3′ (PD); 5′ATCGGGATCCATTTGATTCGAACGATGAGGATGGG3′ and 5′ATCGGGATCCTTAACGTATCTTGTATCTTTTCTTCGCATC3′ (CTD). Because the modeling results were ambiguous as to the exact region of the "thumb" subdomain a second clone of the PD domain which was slightly extended at the C-terminus of the construct was made and termed PD+. The primer pair for this construct was 5′ATCGGGATCCATTCCGTAACTCTGCCGATCGC3′ and 5′ATCGGGATCCTTAAAACCCATCCTCATCGTTCGAATC3′. PCR was carried out using a standard reaction mixture. The amplified DNA fragments were digested with *BamH*I (Fermentas) and ligated into plasmid pET15b (Novagen). Clones with the VP1 fragment in the correct orientation were identified by restriction digest. The resulting expression vectors pET15b NTD, pET15b PD, pET15b CTD and pET15b PD+ were amplified in *E.coli* strain DH5α and verified by sequencing before being introduced into expression strain HMS175 (DE3). The NTD clone spans residues 2-580, the PD clone spans residues 581–896, the CTD clone spans residues 897–1269 and there is no overlap between the PD clone and the CTD clones. The PD+ clone spans residues residues 581–905 and does overlap with the CTD clone.

## Expression and Purification of VP1 Fragments from *E. coli*

Fragments were expressed for 4 h at 30°C in *E.coli* strain HMS174 (DE3) using 1 m*M* IPTG. Cell pellets were resuspended in 1/10 volume of lysis buffer (50 m*M* $NaH_2PO_4$ pH 8.0, 100 m*M* NaCl, 10% glycerol, 1 m*M* BME) and lysed on ice by sonication. Lysates were cleared by centrifugation at 3500 g for 10 min, and the His tagged protein purified as previously described for wild-type VP1 using HIS-SelectTM Cobalt Affinity Gel (Sigma).[17] The identities of the fragments were confirmed by Western blotting and subsequent detection with a mouse monoclonal anti-polyhistidine antibody (Sigma). Replicase assays and NTP binding assays were always performed using freshly made protein.

## NTP Binding

[α-$^{32}$P] CTP (3000 Ci/mmol) was oxidized with 0.5 m*M* sodium periodate in darkness for 20 minutes. Excess periodate was consumed by further incubation in the presence of glycerol. 0.5 μg of protein was mixed with 0.5 μ*M* ox-CTP in 50 m*M* Tris-HCl pH7.5, 6 m*M* magnesium acetate, 0.6 m*M* manganese (II) chloride, 1 m*M* DTT, 2% w/v PEG4000, 7.5*M* sodium cyanoborohydride and the cross-linking reaction was allowed to proceed overnight on ice. The incubation was stopped by the addition of SDS-PAGE loading buffer and the samples electrophoresed on a 12% SDS-PAGE gel. The gel was dried and NTP binding was detected using a Molecular Dynamics Storm 840 phosporimager.[38,39]

## Replicase Activity Assay

Replicase activity was assayed as previously described.[17] Briefly, protein was mixed with a ssRNA template in the presence of NTPs, $Mg^{2+}$ and [α-$^{32}$P] CTP (3000 Ci/mmol) was included in the reaction. The following changes were made to the original assay described by Boyce et al.[17]; actinomycin D was omitted from the reaction, 0.6 m*M* $Mn(II)Cl_2$ was included and the concentration of unlabeled CTP was reduced from 4 to 2 μ*M*. The template used was a T7 transcript identical to the plus strand of BTV segment 10. The dsRNA products of the reaction were electrophoresed on a 9% polyacrylamide gel and detected using a Molecular Dynamics Storm 840 phosporimager.

We thank Nora Cronin at the Department of Crystallography, Birkbeck College, for assistance with the program MODELLER, Craig Williams for helping with the art work, and Geoff Sutton at the Wellcome Trust Centre for Human Genetics, Oxford, for his help in generating the Espript figures.

## REFERENCES

1. Hansen, J. L.; Long, A. M.; Schultz, S. C. Structure 1997, 5, 1109–1122.
2. Bressanelli, S.; Tomei, L.; Roussel, A.; Incitti, I.; Vitale, R. L.; Mathieu, M.; De Francesco, R.; Rey, F. A. Proc Natl Acad Sci USA 1999, 96, 13034–13039.
3. Ng, K. S.; Cherney, M. M.; Lopez Vazquez, A.; Machin, A.; Martin Alonso, J. M.; Parra, F.; James, M. N. G. J Biol Chem 2002, 277, 1381–1387.
4. Butcher, S. J. M. G. J.; Makeyev, E. V.; Bamford, D. H.; Stuart, D. I. Nature 2001, 410, 235–240.
5. Ferrer-Orta, C.; Arias, A.; Perez-Luque, R.; Escarmis, C.; Domingo, E.; Verdaguer, N. J Biol Chem 2004, 279, 47212–47221.
6. Choi, K. H.; Groarke, J. M.; Young, D. C.; Kuhn, R. J.; Smith, J. L.; Pevear, D. C.; Rossmann, M. G. Proc Natl Acad Sci USA 2004, 101, 4425–4430.
7. Appleby, T. C.; Luecke, H.; Shim, J. H.; Wu, J. Z.; Cheney, I. W.; Zhong, W.; Vogeley, L.; Hong, Z.; Yao, N. J Virol 2005, 79, 277–288.
8. Tao, Y.; Farsetta, D. L.; Nibert, M. L.; Harrison, S. C. Cell 2002, 111, 733–745.
9. Koonin, E. V. J Gen Virol 1991, 72 (Pt. 9), 2197–2206.
10. Bruenn, J. A. Nucleic Acids Res 2003, 31, 1821–1829.
11. Bruenn, J. A. Nucleic Acids Res 1991, 19, 217–226.
12. O'Reilly, E. K.; Kao, C. C. Virology 1998, 252, 287–303.
13. Grimes, J. M.; Jakana, J.; Ghosh, M.; Basak, A. K.; Roy, P.; Chiu, W.; Stuart, D. I.; Prasad, B. V. V. Structure 1997, 5, 885–893.
14. Grimes, J. M.; Burroughs, J. N.; Gouet, P.; Diprose, J. M.; Malby, R.; Zientara, S.; Mertens, P. P. C.; Stuart, D. I. Nature 1998, 395, 470–478.
15. Roy, P.; Gorman, B. M. Bluetongue Viruses; Springer-Verlag: Heidelberg, 1990.
16. Urakawa, T.; Ritter, D. G.; Roy, P. Nucleic Acids Res 1989, 17, 7395–7401.

17. Boyce, M.; Wehrfritz, J.; Noad, R.; Roy, P. J Virol 2004, 78, 3994–4002.
18. Makeyev, E. V.; Bamford, D. H. EMBO J 2000, 19, 124–133.
19. Makeyev, E. V.; Bamford, D. H. EMBO J 2000, 19, 6275–6284.
20. Stauber, N.; Martinez-Costas, J.; Sutton, G.; Monastyrskaya, K.; Roy, P. J Virol 1997, 71, 7220–7226.
21. McGuffinLJ, B. K.; Jones, D. T. Bioinformatics 2000, 16, 404–405.
22. Gouet, P.; Diprose, J. M.; Grimes, J. M.; Malby, R.; Burroughs, J. N.; Zientara, S.; Stuart, D. I.; Mertens, P. P. Cell 1999, 97, 481–490.
23. Sali, A.; Potterton, L.; Yuan, F.; van Vlijmen, H.; Karplus, M. Proteins 1995, 23, 318–326.
24. Shi, J.; Blundell, T. L.; Mizuguchi, K. J Mol Biol 2001, 310, 243–257.
25. Stuart, D. I.; Levine, M.; Muirhead, H.; Stammers, D. K. J Mol Biol 1979, 134, 109–142.
26. Cheng, A.; Zhang, W.; Xie, Y.; Jiang, W.; Arnold, E.; Sarafianos, S. G.; Ding, J. Virology 2005, 335, 165–176.
27. Kobayashi, M. T. K. Nagata, K.; Ishihama, A. Virus Res 1992, 22, 235–245.
28. Deng, T. S. J.; Fodor, E.; Brownlee, G. G. J Virol 2005, 79, 8669–8674.
29. Zhang, W. A. N. E. J. J Biol Chem 2001, 276, 2503–2508.
30. Roy, P. Towards the Control of Emerging Bluetongue Disease; Oxford Virology: London, 1991.
31. Cohen, J.; Charpilienne, A.; Chilmonczyk, S.; Estes, M. K. Virology 1989, 171, 131–140.
32. Nason, E.; Rothnagel, R.; Muknerge, S. K.; Kar, A. K.; Forzan, M.; Prasad, B. V. V.; Roy, P. J Virol 2004, 78, 8059–8067.
33. Chenna, R.; Sugawara, H.; Koike, T.; Lopez, R.; Gibson, T. J.; Higgins, D. G.; Thompson, J. D. Nucleic Acids Res 2003, 31, 3497–3500.
34. Kabsch, W.; Sander, C. FEBS Lett 1983, 155, 179–182.
35. Weiner, M. P. C. G. L.; Schoelttin, W.; Cline, J.; Mathur, E.; amd Bauer, J. C. Gene 1994, 151, 119–123.
36. Matsuura, Y.; Possee, R. D.; Overton, H. A.; Bishop, D. H. L. J Gen Virol 1987, 68, 1233–1250.
37. Zhao, Y.; Chapman, D. A.; Jones, I. M. Nucleic Acids Res 2003, 31, E6–6.
38. Stauber, N.; Martinez-Costas, J.; Sutton, G.; Monastyrskaya, K.; Roy, P. J Virol 1997, 71, 7220–7226.
39. Clertant, P.; Cuzin, F. J Biol Chem 1982, 257, 6300–6305.

*Reviewing Editor: Alfred Wittinghofer*